2016

Climatology, Synoptic Conditions, and Misanalyses of Mississippi River Valley Drylines

Rebecca S. Duell

Matthew S. Van Den Broeke

Climatology, Synoptic Conditions, and Misanalyses of Mississippi River Valley Drylines

REBECCA S. DUELL AND MATTHEW S. VAN DEN BROEKE

Department of Earth and Atmospheric Sciences, University of Nebraska–Lincoln, Lincoln, Nebraska

(Manuscript received 24 March 2015, in final form 16 November 2015)

ABSTRACT

The dryline is an important focal point for convection initiation. Although drylines most commonly occur on the southern Great Plains, dryline passages and subsequent severe weather outbreaks have been documented in the Mississippi River valley. This study presents a 15-yr (1999–2013) climatology of these Mississippi River valley drylines and associated severe weather. Additionally, synoptic patterns are identified that may result in drylines moving atypically far eastward into the Mississippi River valley. In total, 39 Mississippi River valley drylines (hereafter referred to as MRV drylines) were identified from the North American Regional Reanalysis (NARR) dataset through the study period. Mean and anomaly synoptic composites were created for these drylines. MRV dryline events typically occur under synoptically active conditions with an amplified upper-air pattern, a 500-hPa shortwave trough to the west or northwest of the dryline, and a strong surface cyclone to the north. These boundaries are often misanalyzed or inconsistently analyzed as cold fronts, stationary fronts, or trough axes on surface maps; of the 33 cases of identified MRV drylines for which the Weather Prediction Center archived analyses were available, only 6 were correctly analyzed as drylines. Drylines moving into the Mississippi River valley often result in severe weather outbreaks in the Mississippi River valley, the Midwest, and the southeastern United States.

1. Introduction

The dryline is an airmass boundary marked by a strong moisture gradient. In the United States, the dryline typically sets up meridionally over the Great Plains during spring and marks the boundary between hot, dry air from the Mexican Plateau and warm, moist air originating over the Gulf of Mexico. The dryline tends to be a zone of enhanced convergence, which makes it a focal point for convection initiation (e.g., Rhea 1966; Schaefer 1974, 1986; Hane et al. 1997; Atkins et al. 1998; Ziegler and Rasmussen 1998; Hoch and Markowski 2005; Weiss et al. 2006; Schultz et al. 2007).

Schultz et al. (2007) created a 2-yr springtime climatology of west Texas drylines and identified synoptic-scale patterns that regulate dryline intensity. Their results showed that the strongest drylines in western Texas had a composite 250-hPa jet maximum of 25–30 m s^{-1} over the eastern Pacific Ocean, a composite 500-hPa slightly negative-tilted shortwave trough over the western United States approaching Texas, and a composite surface cyclone over eastern New Mexico and western Texas. In contrast, weak drylines had a composite 250-hPa jet located farther poleward over the north-central United States and central Canada, a composite 500-hPa ridge over the central United States, and a broader composite area of surface low pressure over the southwestern United States and northwestern Mexico. Schultz et al. (2007) addressed synoptic conditions that contribute to dryline intensity, though the literature is relatively quiet on synoptic patterns that result in drylines moving atypically far eastward. This study builds on Schultz et al. (2007) by adding Mississippi River valley (MRV) dryline events and retaining a synoptic-scale focus.

A number of dryline climatologies have been published (e.g., Rhea 1966; Schaefer 1974; Hoch and Markowski 2005; Schultz et al. 2007), though none of them extend east of the Great Plains. These studies examined April–June, climatologically the most active time for southern plains drylines. Dryline placement at 0000 UTC peaks near 101°W, with drylines "becoming rare east of 95°W" (Hoch and Markowski 2005).

Significant tornadoes and tornado outbreaks east of the Great Plains have occurred on days when a MRV

Corresponding author address: Rebecca S. Duell, National Weather Service Anchorage Forecast Office, 6930 Sand Lake Road, Anchorage, AK 99502.
E-mail: rebecca.duell@noaa.gov

DOI: 10.1175/MWR-D-15-0108.1

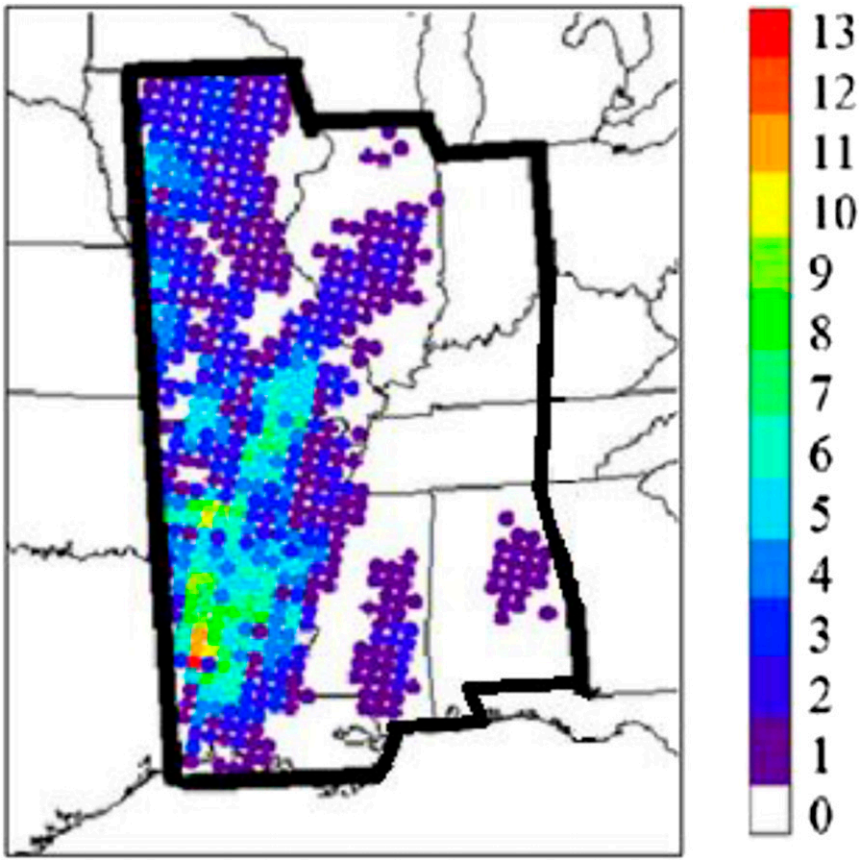

FIG. 1. Dryline days identified per point, with study domain approximately indicated by the black outline. All values indicate dryline days identified by computer algorithm, after quality control.

dryline was present. On 18 March 1925, the single deadliest tornado in U.S. history, the Tristate tornado, occurred when a dryline progressed eastward into southern Illinois (Maddox et al. 2013). In this event, an inversion aloft in the warm sector [characteristic of warm sectors ahead of drylines due to the typical eastward slope of a dryline with height; Maddox et al. (2013)] initially suppressed deep convection initiation, allowing for the supercell that produced the Tristate tornado to remain isolated and largely uninfluenced by interactions with other storms. The Super Outbreak of 1974 (e.g., Miller and Sanders 1980; Locatelli et al. 2002b; Corfidi et al. 2010) occurred on a day when the dryline moved into southeastern Missouri and southern Illinois. Most of the violent tornadoes during this event were associated with a second squall line, which was spawned when a cold front aloft occluded with the dryline (Locatelli et al. 2002b). More recently, one of the most significant tornado outbreaks in the past 50 years, the 27 April 2011 outbreak, occurred on a day when the dryline moved into central Arkansas. Though uncommon, such cases illustrate that a dryline can move into the Mississippi River valley, which has resulted in substantial severe weather outbreaks. However, little is known about how often and under what circumstances these drylines move atypically far eastward. Thus, this study has two primary objectives:

1) Present a 15-yr climatology (1999–2013) of dryline passages for the Mississippi River valley and discuss how often these events are associated with reports of severe weather.
2) Describe typical synoptic patterns associated with drylines affecting the Mississippi River valley region.

2. Data and methodology

A computer algorithm was developed to identify points along drylines in the study's domain, which included Louisiana, Arkansas, Missouri, Iowa, Illinois, Indiana, Mississippi, and Alabama, and western parts of Kentucky and Tennessee (domain outlined with thick black line in Fig. 1). The algorithm used data from the National Centers for Environmental Prediction (NCEP) North American Regional Reanalysis (NARR) dataset

(Mesinger et al. 2006). This is a 32-km horizontal grid spacing 3-hourly atmospheric and land surface hydrology dataset for the North American domain. For this project, all NARR data points within the study domain at all NARR hours (0000, 0300, 0600, 0900, 1200, 1500, 1800, and 2100 UTC) were examined on each day within the 15-yr study period (1999–2013). The algorithm flagged geographic points that met a set of three dryline identification criteria: a specific humidity gradient requirement, a wind directional requirement, and a maximum temperature gradient requirement. Consistent with the approach of Hoch and Markowski (2005), a specific humidity gradient of at least $3 \times 10^{-8}\,\mathrm{m}^{-1}$ [$3\,\mathrm{g\,kg}^{-1}\,(100\,\mathrm{km})^{-1}$] was the first requirement utilized by the algorithm. This specific humidity gradient was required to point with an eastward component, ensuring that the air mass to the east of the boundary had higher moisture content. Because both drylines and frontal boundaries will exhibit a moisture gradient, the second and third criteria were added in order to distinguish drylines from frontal boundaries. The second criterion specified a range of wind directions from 50 km east of to 50 km west of the points. Winds to the east of the point were required to be from between 80° and 190°, whereas winds to the west of the point were required to be from between 170° and 280°. This wind shift from southerly or southeasterly to westerly or southwesterly is typical of the wind shift across a dryline and eliminates any cold fronts that have a strong northerly component to the advancing polar air mass. The final algorithm criterion was that the temperature gradient must be less than $+0.02^{\circ}\mathrm{C\,km}^{-1}$ from west to east across a point. Because the dryline is an airmass boundary between two tropical air masses [continental tropical (cT) and maritime tropical (mT)], the temperature gradient across the boundary should be fairly small in comparison with a typical cold front. Identified cases were also individually examined to exclude contamination by convection (e.g., Schultz et al. 2007) through radar analysis. Time-of-day criteria were not included as in some past studies (e.g., Schaefer 1974; Schultz et al. 2007), because MRV drylines typically occur in synoptically active environments and are not as closely tied to the diurnal cycle as the high plains drylines that more frequently occur in quiescent environments. In compiling the final number of dryline passages per state and per point, presented in section 3, points that were flagged multiple times per day due to the 3-hourly NARR temporal resolution were only counted once in the final dryline count per state or per point.

Air parcels on either side of algorithm-flagged drylines were run through the National Oceanic and Atmospheric Administration (NOAA) Air Resources Laboratory Hybrid Single-Particle Lagrangian Integrated Trajectory (HYSPLIT) model (Draxler and Hess 1997, 1998; Draxler 1999; Draxler and Rolph 2015; Rolph 2015) using the 32-km horizontal grid spacing 3-hourly NARR dataset to verify origins of air parcels on both sides of the boundaries. If parcels west of the boundary originated from the Mexican Plateau and parcels east of the boundary originated from the Gulf of Mexico, then the boundary was included in this study's database of MRV dryline events. For this study, the Mexican Plateau was subjectively defined as the region of the southwestern United States and northwestern Mexico that has a hot arid climate. This generally encompassed northwestern Mexico, and southern New Mexico, Arizona, and California. Once MRV drylines were identified, associated synoptic patterns were analyzed.

Composite synoptic fields were constructed using the NCEP–National Center for Atmospheric Research (NCAR) reanalysis dataset (Kalnay et al. 1996) archived by the NOAA/Earth System Research Laboratory (ESRL). Composite images (see Fig. 7) were provided by the NOAA/ESRL Physical Sciences Division, Boulder, Colorado, from their website at http://www.esrl.noaa.gov/psd/. Variables analyzed were 250-hPa vector wind and anomaly, 500-hPa geopotential height and anomaly, 850-hPa zonal wind and anomaly, and mean sea level pressure. For each variable, mean and anomaly composites were created using all 39 dryline days at the time of the event, chosen as the time when the dryline progressed farthest east. Anomalies were calculated relative to each day's 30-yr (1981–2010) mean.

3. Climatology results

a. Computer algorithm results

The number of dryline passages per point as identified by the computer algorithm after quality control is plotted in Fig. 1. The highest number of dryline passages per point identified by the algorithm generally occurred in northwest Louisiana and southwest Arkansas.

The points that were identified by the algorithm (Fig. 1) occasionally appear in an isolated or somewhat isolated group of points from the points farther west (i.e., the points in Mississippi, Alabama, and Illinois). Although synoptically active drylines have been shown to exhibit discontinuous motion at times (Hane 2004), there are other possible explanations for the apparent stepwise movement of the boundaries that highlight some limitations of the algorithm. Individual analysis of the movement of the drylines that contained gaps in the algorithm identification revealed that these gaps tended to occur in the overnight hours. It is likely in these instances that a weaker boundary was still present overnight between the identified points and was moving

eastward; however, it was not identified by the algorithm because either the maximum temperature gradient threshold was exceeded [due to the diurnal reversal and strengthening of the temperature gradient across a dryline (e.g., Geerts 2008)] or the specific humidity gradient criterion was not met. The specific humidity gradient could be slightly weaker overnight due to the lack of localized turbulent mixing of the elevated mixed layer (EML) west of the boundary in the overnight hours. The apparent difficulty in algorithm identification of nocturnal drylines shows a limitation in using a single set of criteria to identify drylines at all hours of the day, as nocturnal drylines tend to more strongly resemble cold fronts than daytime drylines due to the diurnal cooling of the cT air mass. Additionally, the apparent stepwise movement of the drylines could also be attributed to a limitation of the dataset used in the study—the 3-hourly temporal interval of the NARR dataset. When drylines moved rapidly eastward, points passed over by the dryline between NARR hours were not flagged.

Because of these limitations, the algorithm was unable to flag all of the points along the drylines. Therefore, it is likely that the number of dryline passages per point identified by the algorithm (Fig. 1) is slightly underrepresentative of the actual number of dryline passages at each point. To test the algorithm before the climatology was compiled, 14 MRV drylines were identified from surface map analysis and the days were run through the identification algorithm. All of the test drylines were flagged when the program was run, leading the authors to believe that if any MRV drylines were excluded, the number of missed events was small.

b. *Mississippi River valley dryline climatology and association with severe weather*

A total of 39 MRV drylines were identified between 1999 and 2013. A graphical representation of the number of dryline passages identified through each state is shown in Fig. 2. By state, Arkansas had the most drylines (19), followed by Louisiana (15) and Missouri (12). Drylines move into Louisiana, Arkansas, and Missouri approximately annually, and farther east approximately once per decade.

Studies of Great Plains drylines have found that drylines occur most often in late May and June (Hoch and Markowski 2005; Schultz et al. 2007). MRV drylines peak earlier in the year, between February and April (Fig. 3). No drylines were observed in the study domain between July and September. The absence of drylines during these months may be partially attributed to the typical moistening of the air over the southwestern United States during July, August, and September (Robinson 1998), and may also reflect the rarity of strong midlatitude cyclones and accompanying strong westerly momentum aloft in the region.

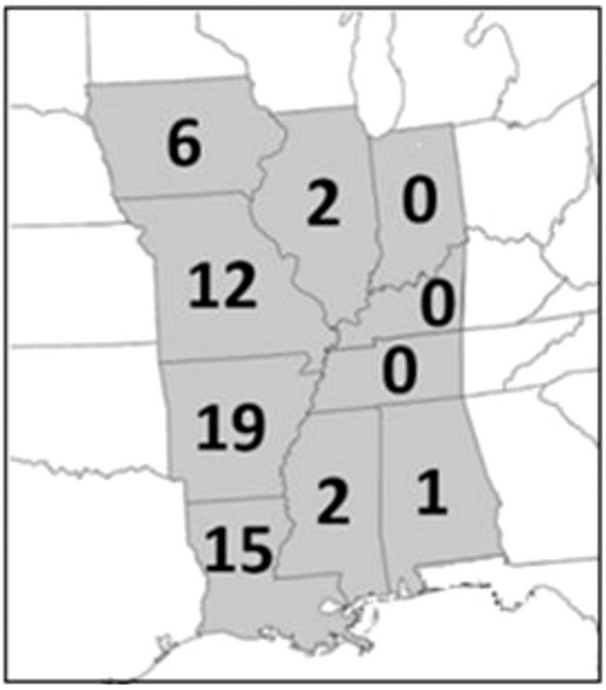

FIG. 2. Number of dryline days for each state from 1999 to 2013.

Figure 4a shows the easternmost longitude at which each dryline was analyzed throughout the MRV dryline season (October–June). The drylines in the study moved farther east during late winter and early spring (easternmost longitude 86°–91°W), and not as far east during fall and late spring (easternmost longitude 91°–95°W). There were no observed drylines east of 90°W except in January, February, and March (Fig. 4a). Figure 4b shows the northernmost latitude of each dryline throughout the MRV dryline season. The northernmost latitude of MRV drylines increased from approximately 32°–34° to 40°–42°N through the MRV dryline season—MRV drylines are generally located farther south in late fall and winter, and farther north in spring. Throughout the time when MRV dryline events occurred, some were present southward to the southern border of the study domain (Figs. 1 and 4b).

The shift in mean MRV dryline location toward higher latitudes in May and June is likely partially due to the northward shift in mean extratropical cyclone track throughout the dryline season (e.g., Eichler and Higgins 2006). Because MRV drylines occur under active synoptic patterns and are strongly tied to a surface cyclone, it follows that their mean location would shift northward through the spring as the mean path of surface cyclones shifts northward (e.g., Dos Santos Mesquita et al. 2008). Some cyclones track relatively far south even during the late spring and early summer, resulting in a few MRV

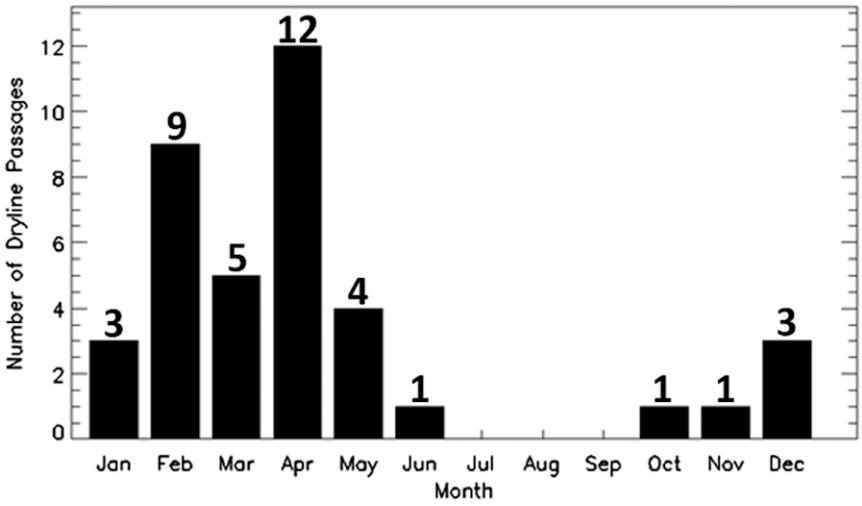

FIG. 3. Number of MRV dryline events per month.

drylines near the southern border of the study domain throughout the MRV dryline season (Fig. 4b).

Events when a dryline travels into the Mississippi River valley have been associated with severe weather outbreaks. For the sample of 39 MRV dryline events identified in this study, corresponding reports of tornadoes and severe-criteria hail and convective wind were gathered from the Storm Events Database published by the National Climatic Data Center (NOAA/National Centers for Environmental Information 2015). Reports were gathered from the state(s) in which the algorithm flagged a dryline, and it was ensured that reports corresponded to when and where the dryline was active. This methodology will miss events in other states associated with the same boundary, but helps ensure that included storm reports are associated with the algorithm-identified dryline. The Storm Events Database has known limitations (e.g., Doswell et al. 2005; Trapp et al. 2006), including temporal offset between reports and actual severe weather events, and missed events. Temporal offset does not influence our results, though the potential absence of wind, hail, or tornado reports may. Geographically differing verification procedures may also influence the results—for instance, some forecast offices aggressively collect reports of severe weather, while others may not (e.g., Smith 1999).

In total 21 (54%) of the 39 of MRV dryline events were associated with severe weather reports in the state(s) in which the dryline was identified. Just over half of MRV dryline days were associated with regional severe weather outbreaks, likely reflecting the synoptically active nature of these events. The state with an algorithm-identified dryline was typically the westernmost state with severe weather reports on a given day. For instance, on the 27 April 2011 southeastern outbreak (e.g., Knupp et al. 2014), the dryline-flagged states of Louisiana and Arkansas had a total of 17 hail reports, 43 wind reports, and 4 tornado reports, which occurred early in the event (not shown). For all MRV dryline events associated with severe weather reports, each was associated with an average of 26 hail reports, 13 wind reports, and 7 tornado reports. The average largest hail size and average maximum reported wind gust associated with these events, respectively, were 5.5 cm and 31.7 m s^{-1}. Of the 15 events with associated tornadoes, 9 (60%) had at least 1 tornado with a rating of F2 or EF-2 or greater. In only 2 cases with severe reports were less than 10 reports received; the median value was 36 and the average value 46. These findings imply that when a MRV dryline is able to initiate deep convection, that convection is often severe, likely owing to the strong vertical wind shear and destabilization commonly occurring with the synoptic pattern with which MRV drylines are associated. The greatest significance of a MRV dryline may be that it serves as an initiator of convection in an already favorable severe weather environment.

4. Eastward movement of cT air

To better understand and provide evidence for the processes that resulted in cT air moving atypically far eastward on MRV dryline days, observed soundings and 60-h backward air parcel trajectories were examined. The observed soundings were taken near the boundary in the hours leading up to and at the time of the dryline passage. The backward air parcel trajectories were modeled with the HYSPLIT model using the NARR 32-km horizontal grid spacing reanalysis data. The time step implemented in HYSPLIT is variable, and requires

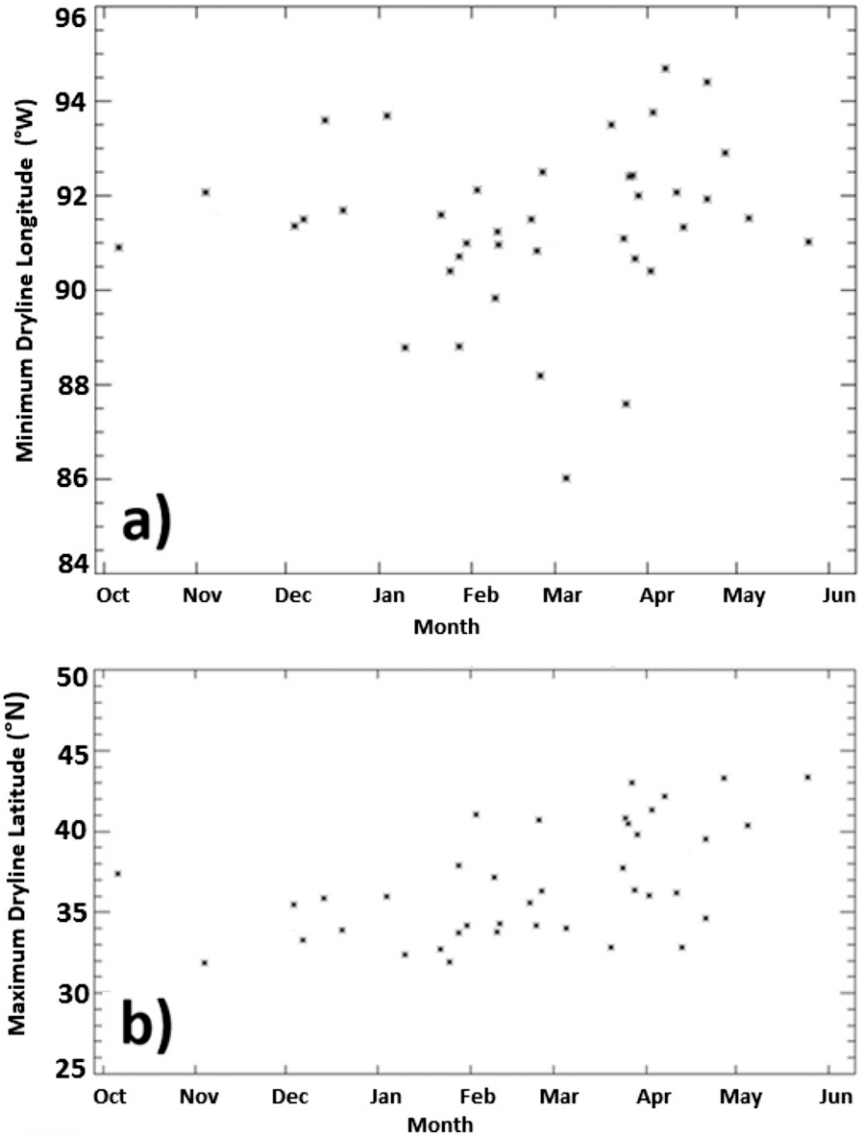

FIG. 4. (a) Easternmost observed dryline longitude for each MRV dryline event. (b) Northernmost observed dryline latitude for each MRV dryline event.

that the advection distance be less than grid spacing. Since the NARR data have 3-h temporal interval, this time step would yield the optimal information from HYSPLIT trajectories. Discrepancies between the temporal resolution of the NARR data and the HYSPLIT time step may increase trajectory uncertainty, but the inclusion of multiple trajectories raises our confidence in the HYSPLIT results.

Of the 27 events in which observed soundings just to the east of the easternmost dryline location were available, the soundings from 17 events showed an EML 12–24 h before the dryline event, which subsequently descended to the surface by the time of the dryline event. The presence of an EML far from its source region has been implicated in significant severe weather events in the northeastern United States (Banacos and Ekster 2010). An example of the EML present on a MRV dryline day is shown in the Lincoln, Illinois (KILX), 1200 UTC 7 April 2001 sounding (Fig. 5a). An EML can be seen from 675 to 500 hPa as a layer with dry adiabatic lapse rates and an increase in environmental relative humidity with height (e.g., Carlson et al. 1983). Below the EML, a strong capping inversion is present. By the time of the dryline event (0000 UTC; Fig. 5b) the capping inversion had disappeared and dry air was present at the surface. Although this may be partially attributed to the descent of dry air, a time series through

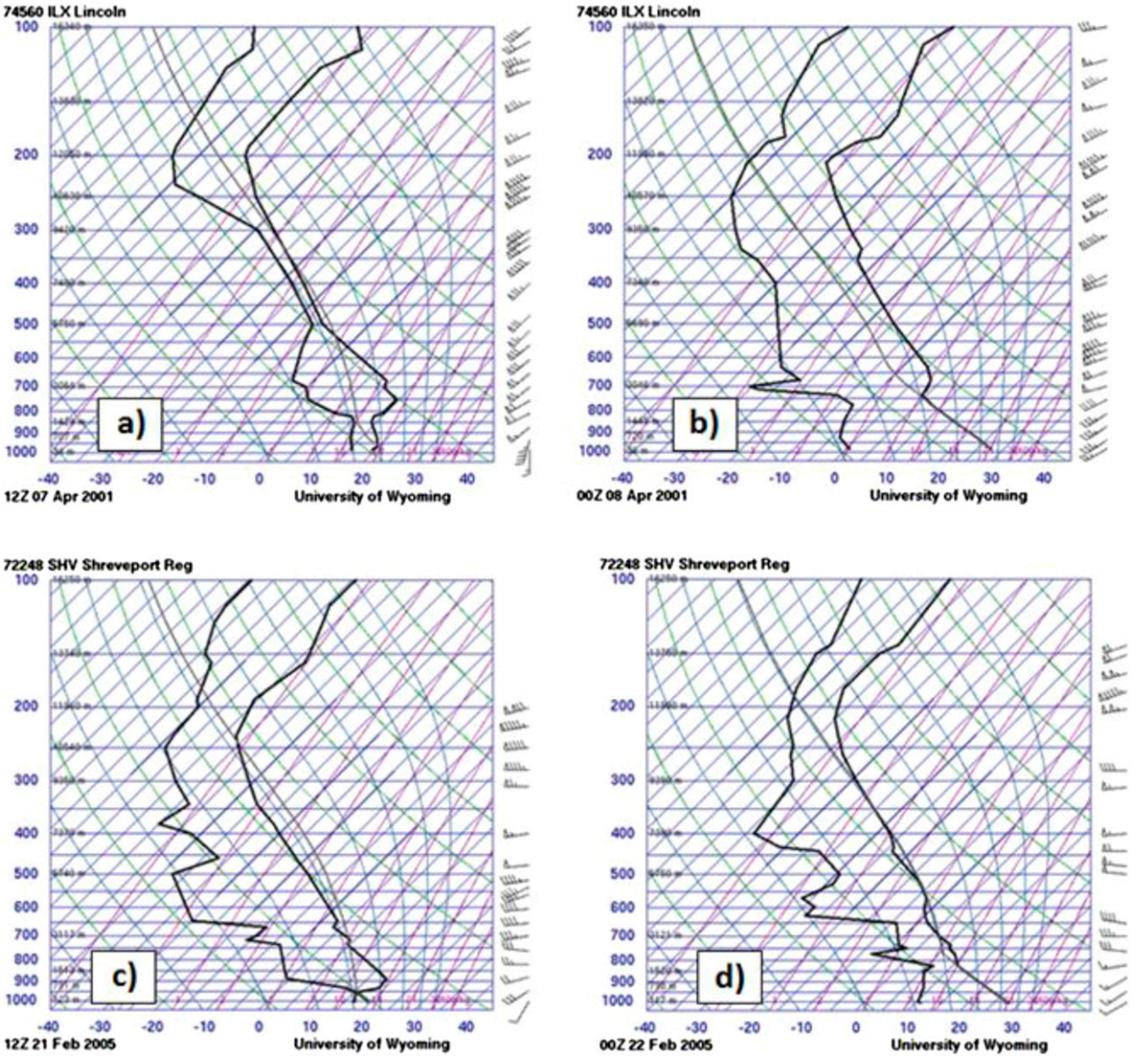

FIG. 5. (a) 1200 UTC 7 Apr 2001 Lincoln, IL (KILX), sounding. (b) 0000 UTC 8 Apr 2001 Lincoln sounding. (c) 1200 UTC 21 Feb 2005 Shreveport, LA (KSHV), sounding. (d) 0000 UTC 22 Feb 2005 Shreveport sounding.

the day also indicated substantial dry air advection at the surface (not shown). Another example of an EML can be seen in the 1200 UTC 21 February 2005 Shreveport, Louisiana (KSHV), observed sounding (Fig. 5c). The EML in this case was between approximately 900 and 750 hPa. Again, a strong capping inversion was present. The 0000 UTC sounding taken at the same location 12 h later (Fig. 5d) shows that the elevated dry layer had descended to the surface. The soundings from these cases were presented because they typified situations in which an EML was present, prior to a MRV dryline event.

Backward air parcel trajectories presented in Fig. 6 show patterns of eastward dry air advection likely contributing to MRV drylines. A 60-h HYSPLIT backward air parcel trajectory from the 23 February 2012 Arkansas dryline (Fig. 6a) shows dry air advection at the 200- and 500-m levels in the 48 h preceding the dryline event. In the 17 February 2011 Iowa dryline (Fig. 6b), the 200-m air in southwestern Iowa appears to have originated to the southwest. During a Missouri dryline event on 16 April 2012 (Fig. 6c) air parcels at 3000 m AGL descended on a synoptic scale to 500 and 200 m AGL in the day preceding the dryline event, while traveling from the southwestern United States.

These air parcel trajectories and the analysis of observed soundings suggest that during MRV dryline

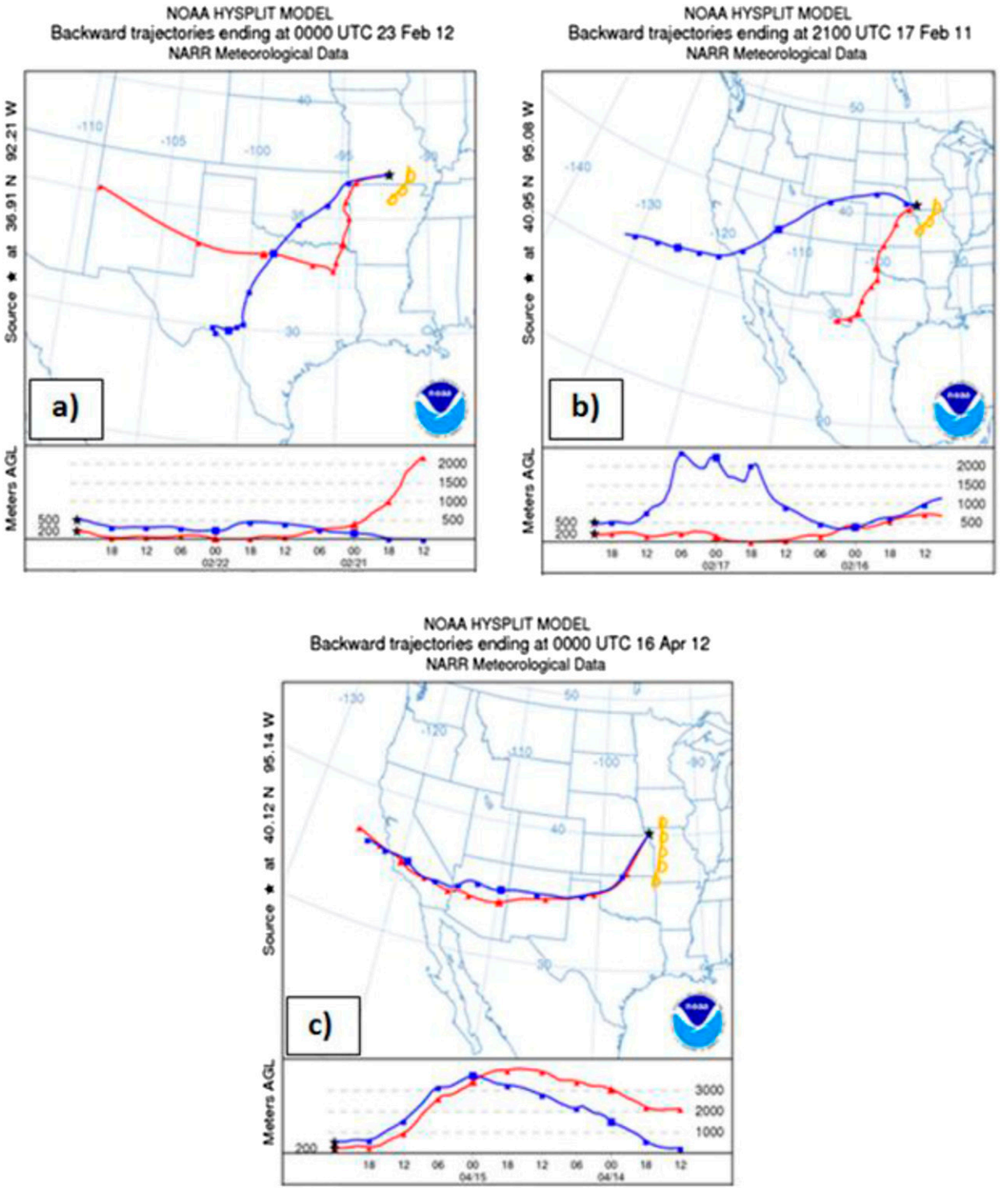

FIG. 6. The 60-h NOAA HYSPLIT model backward air parcel trajectories for air parcels 200 m AGL (red) and 500 m AGL (blue) ending at (a) 0000 UTC 23 Feb 2012, (b) 2100 UTC 17 Feb 2011, and (c) 0000 UTC 16 Apr 2012. Smaller markers are plotted every 6 h, larger markers every 24 h. Approximate surface dryline location at each time is indicated by an orange scalloped boundary.

events, both low-level dry air advection and/or descent of EML air to the surface may contribute to the formation of a surface Mississippi River valley dryline. In some cases, elevated dry air is transported eastward, possibly within an EML, and then appears to descend to the surface either through turbulent mixing or synoptic-scale descent. Eastward transport of dry air aloft within an EML is consistent with the observations of Banacos and Ekster (2010). In other cases, the dry air seems to originate at lower levels and is transported eastward near the surface. Analysis of the observed soundings and the backward air parcel trajectories provided evidence of cases of both low-level dry air advection and descent of an elevated dry layer.

5. Synoptic composites for Mississippi River valley drylines

A common large-scale pattern was identified as favorable for MRV drylines, with generally minor variations in the location and strength of synoptic features by dryline region within the study domain. The composite upper-air pattern on MRV dryline days is highly amplified (Fig. 7a), with strong winds at the base of a trough and downstream from the trough axis across the study domain. Anomalously strong 250-hPa southerly winds were present through much of the Mississippi River valley (Fig. 7b). These composites reveal that MRV drylines are often associated with the polar jet dipping into the southern United States and a composite mean jet streak over or just west of the dryline location (Fig. 7a). In individual cases, the polar and subtropical jets often merged to the east or southeast of the dryline location (not shown). A composite shortwave trough was present to the northwest of MRV drylines (Fig. 7c), with negative composite height anomalies >90 m centered over Kansas and Nebraska (Fig. 7d). Such an amplified upper-air pattern is supportive of large low-level baroclinicity and intense cyclogenesis, and has been observed in previous dryline studies (Rhea 1966; Hoch and Markowski 2005; Schultz et al. 2007). When surface observations were examined for the 39 events identified in this study, 31 (79.5%) were associated with surface cyclones with minimum central pressure ≤1000 hPa, and 21 (53.8%) were associated with surface cyclones with minimum central pressure ≤995 hPa. Baroclinicity was also strong, with 31 events (79.5%) associated with a temperature difference ≥25°C across a box bounded by 85°–105°W and the northern and southern United States borders. Of the 39 cases, 19 events (48.7%) had a temperature difference ≥30°C across the same box.

When drylines move east of their typical Great Plains domain, strong westerly momentum is typically present to the west of the dryline. The composite zonal 850-hPa wind component exceeded 10 m s^{-1} over a large region centered on Arkansas, northern Mississippi, and northern Louisiana (Fig. 7e). This 850-hPa zonal component was anomalously strong (Fig. 7f). This anomalously strong zonal wind indicates substantial westerly momentum available to be mixed to the surface and to move the dryline eastward. Consistent with the synoptic features shown here, MRV drylines were associated with an intense composite surface cyclone (Fig. 7g) centered over Iowa, Illinois, and Missouri. Although the composite cyclone was around 1003 hPa, many individual events were associated with much deeper surface cyclones.

The basic synoptic model of MRV drylines varies most substantially when drylines are identified in Mississippi and Alabama. Days with drylines in this region are marked by a composite 250-hPa jet exceeding 60 m s^{-1}. These drylines are also associated with negative 500-hPa geopotential height anomalies >120 m and a composite surface cyclone <998 hPa (not shown).

Minimum central pressure of the associated surface cyclone was recorded at the time of maximum eastward dryline location for each of the 39 MRV dryline events. These observational data support the composite pattern of an intense surface cyclone, with an average minimum pressure of 997 hPa for Louisiana and Arkansas drylines, 993 hPa for drylines in Missouri/Iowa/Illinois, and 990 hPa for Mississippi and Alabama drylines. In comparisons using a one-tailed Student's t test, the difference in central pressure between Louisiana/Arkansas drylines and Missouri/Iowa/Illinois drylines was statistically significant ($p = 0.009$). The difference between Louisiana/Arkansas and Mississippi/Alabama drylines was also significant ($p = 0.023$), despite only 3 Mississippi/Alabama events. These findings suggest that more intense surface cyclones are typically required as drylines move farther east from their usual Great Plains domain.

Synoptic composites for these MRV drylines are similar to those for strong drylines created by Schultz et al. (2007). Both their composites and our composites for MRV drylines yield an upper-level composite jet maximum >25 m s^{-1} over the eastern Pacific Ocean (Fig. 7a), a 500-hPa composite shortwave trough to the northwest of the dryline (Fig. 7c), and a composite surface cyclone with central pressure <1004 hPa to the north of the dryline (Fig. 7g). MRV dryline days yield markedly deeper composite cyclones than composites of the strong dryline days identified by Schultz et al. (2007).

Caution should be applied when comparing synoptic composites for MRV drylines in different geographic regions, because different numbers of cases were analyzed in each region. Though it appears that deeper

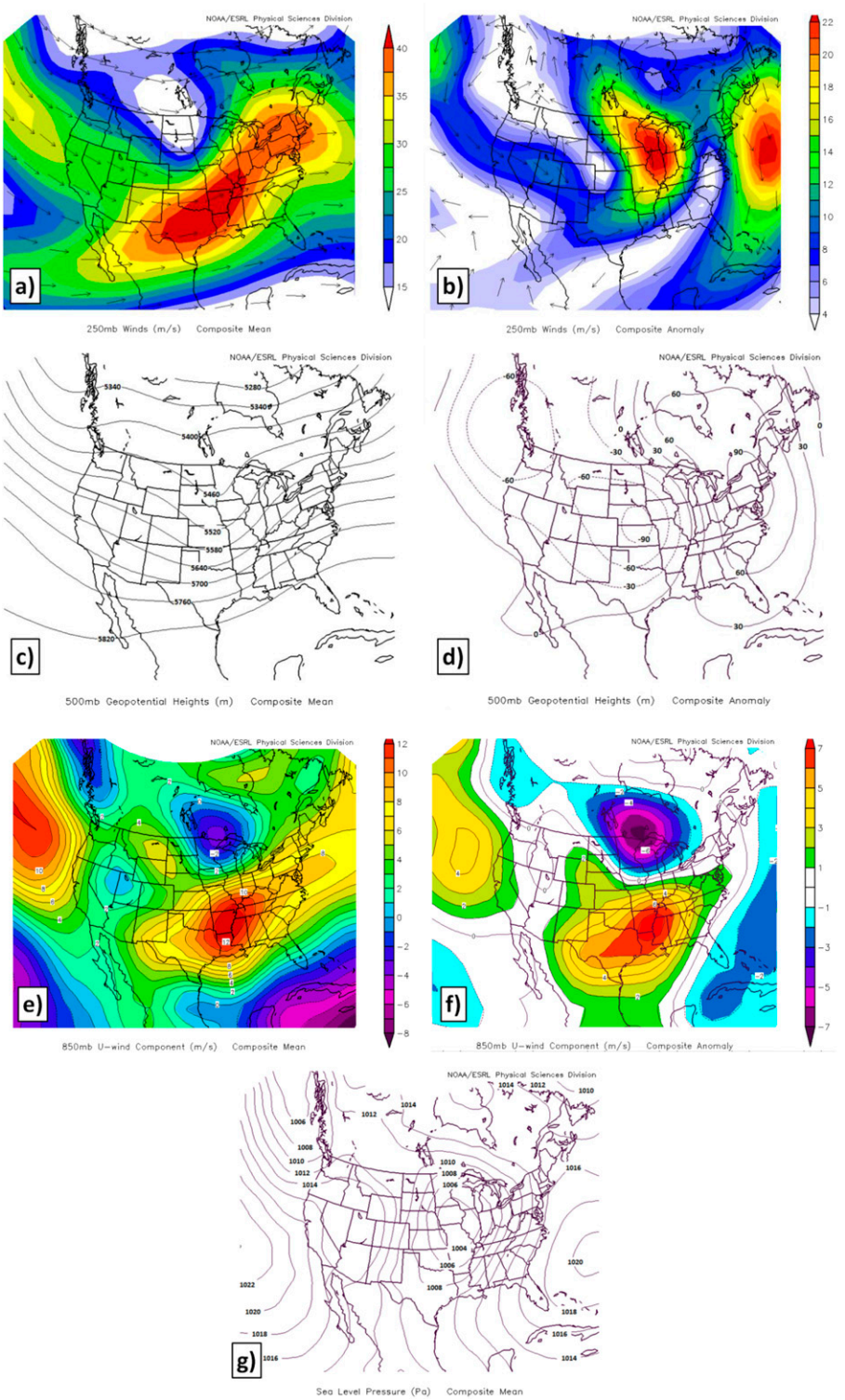

FIG. 7. Synoptic composites at time of easternmost extent for MRV drylines. (a) Mean 250-hPa vector wind ($m\,s^{-1}$), (b) anomaly 250-hPa vector wind ($m\,s^{-1}$), (c) mean 500-hPa geopotential height (m), (d) anomaly 500-hPa geopotential height (m), (e) mean 850-hPa zonal wind component ($m\,s^{-1}$), (f) anomaly 850-hPa zonal wind component ($m\,s^{-1}$), and (g) mean sea level pressure (hPa). Composites were created using all 39 MRV dryline events identified, at the hour at which the maximum eastward location occurred.

surface cyclones and stronger 300-hPa jet streaks are present when drylines move into Mississippi and/or Alabama, only three cases in this region cannot strongly support climatological conclusions.

6. Mississippi River valley dryline analyses on surface maps

Drylines that move atypically far eastward are often misanalyzed on surface frontal analyses. Hobbs et al. (1996) noted that for cyclones in the lee of the Rocky Mountains, dry troughs [surface pressure troughs that have the characteristics of both a dryline and a lee trough; Martin et al. (1995)] are often misanalyzed as cold fronts. This is a mistake that can result from the misuse of the Norwegian cyclone model to describe cyclones in the central United States. Three typical examples are presented to illustrate dryline misanalyses (24–25 February 2007, 11 February 2009, and 2 April 2010). Surface maps analyzed by the Weather Prediction Center [(WPC); then the Hydrometeorological Prediction Center] are shown in Figs. 8a, 9a, and 10a, maps with station plots and color-contoured dewpoint are included in Figs. 8b, 9b, and 10b, and HYSPLIT backward air parcel trajectories are shown for these cases in Figs. 8c, 8d, 9c, 9d, 10c, and 10d. The 60-h backward air parcel trajectories in Figs. 8c, 9c, and 10c are taken from three different points around the cyclone, illustrating the presence of air from typical continental polar (cP), cT, and mT source regions in the corresponding sectors of a cyclone. The 60-h backward air parcel trajectories initialized over a rectangular grid of points, shown in Figs. 8d, 9d, and 10d, support the representativeness of points used in Figs. 8c, 9c, and 10c.

The 0300 UTC 25 February 2007 WPC weather map analysis of the first example, 24–25 February 2007, has a double-front cyclone analyzed in eastern Kansas (Fig. 8a). Mulqueen and Schultz (2015) showed that double-front cyclones, though differing from the Norwegian cyclone model, are common structures in cyclones over the eastern North Atlantic. However, analysis of the evolution of this weather system and the source of the air parcels in each air mass confirms that this is not a double-front cyclone, but rather a typical lee cyclone (Hobbs et al. 1996) with a dryline and an arctic front. The low began as a lee cyclone in northeastern New Mexico. As the low tracked eastward and deepened, two boundaries extended equatorward from the cyclone. Backward air parcel trajectories (Figs. 8c and 8d) show three distinct airmass source regions south of the cyclone. The air mass farthest east ahead of the first analyzed cold front originated over the Gulf of Mexico (Figs. 8c and 8d) and was warm and humid, typical of mT air (Fig. 8b). The second air mass between the two analyzed cold fronts originated over the southwestern United States (Figs. 8c and 8d), and was characterized by high temperature and low dewpoint (Fig. 8b). The strong dewpoint gradient through Louisiana and eastern Arkansas (Fig. 8b) is therefore a boundary between cT and mT air, and thus is a dryline rather than a cold front as analyzed in Fig. 8a.

In the second example (11 February 2009), a lee cyclone developed in southern Colorado on the afternoon of 10 February 2009. The cyclone strengthened to 990 hPa as it moved eastward into the Mississippi River valley on the afternoon of 11 February 2009 (Fig. 9a). The surface observations in the 24 h leading up to 1800 UTC (not shown) indicate three distinct air masses associated with the cyclone: a mT air mass to the east with high temperature and high dewpoint, a cT air mass to the south with high temperature and low dewpoint, and a cP air mass to the northwest with low temperature and low dewpoint. By 1800 UTC 11 February 2009, these three distinct air masses were still visible in surface observations (Fig. 9b). The boundary analyzed as a cold front stretching from western Illinois to southwestern Louisiana and into the Gulf of Mexico (Fig. 9a) is the boundary between warm, moist mT air to the east and warm, dry cT air to the west. This defines the boundary as a dryline. The trough extending to the southwest from the surface cyclone is a boundary between warm, dry cT air and cold, dry cP air, and is thus a cold front. Backward air parcel trajectories from HYSPLIT (Figs. 9c and 9d) confirm the origins of the air masses, demonstrating that the cP air mass originated over Canada, the cT air mass traveled eastward from the southwestern United States, and the mT air mass traveled northward from the Gulf of Mexico.

Finally, a third example (2 April 2010) highlights a lee trough that transitioned into a dryline. A cyclone developed in a lee trough extending southward through eastern New Mexico and southwestern Texas on 1 April 2010. A lee trough is a favorable location for dryline development due to the confluent wind field that helps to focus a broad low-level specific humidity gradient (Steenburgh and Mass 1994). Steenburgh and Mass (1994) pointed out that not all lee troughs become drylines; specifically, lee troughs in the winter that often have polar air masses to the east do not exhibit the characteristics of a dryline. However, during the spring months when the zonal moisture gradient increases due to increased northward moisture transport off the Gulf of Mexico and an increased vegetation and associated evapotranspiration gradient, lee troughs often sharpen the moisture gradient enough through confluent deformation and convergence that a dryline develops

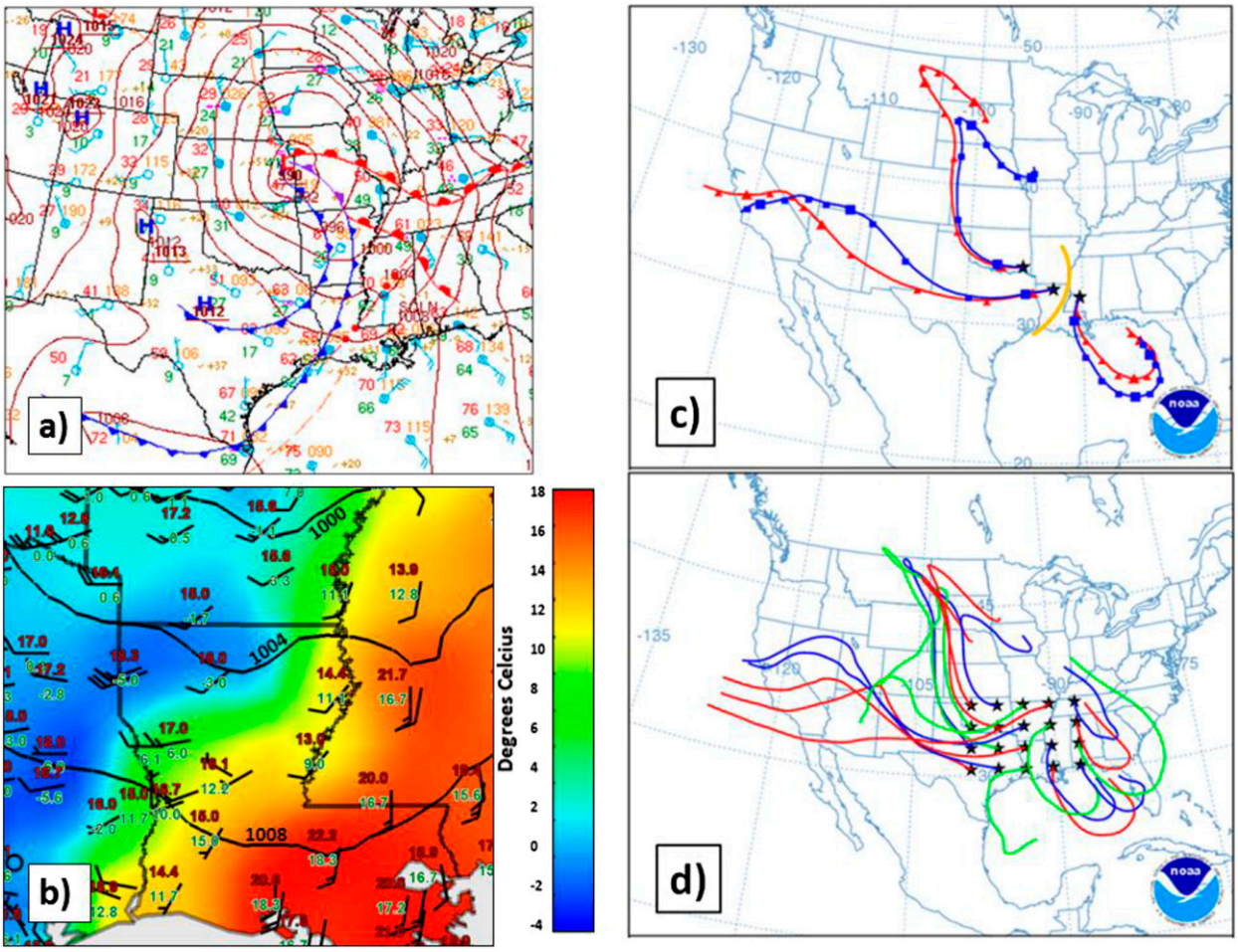

FIG. 8. (a) Weather Prediction Center surface analysis for 0300 UTC 25 Feb 2007. (b) Surface observations at 0300 UTC 25 Feb 2007. Station plot temperature and dewpoint in °C and wind in kt (full barb = 5 m s^{-1}; half barb = 2.5 m s^{-1}). Dewpoint is color shaded, and black contours represent surface pressure (interval 4 hPa). Note the strong dewpoint gradient in northern Louisiana/eastern Arkansas, with increasing dewpoint northwestward. Observations plotted using WeatherScope from the Oklahoma Climatological Survey. (c) The 60-h HYSPLIT backward air parcel trajectories for 200 m AGL (red) and 500 m AGL (blue) for 0300 UTC 25 Feb 2007. Smaller markers are plotted every 6 h and larger markers are plotted every 24 h. The approximate dryline location is denoted by an orange line. (d) The 60-h matrix HYSPLIT backward air parcel trajectories for 300 m AGL for 0300 UTC 25 Feb 2007.

(Steenburgh and Mass 1994; Schultz et al. 2007). On 1 April 2010, the dryline that had developed from the lee trough over eastern New Mexico progressed northeastward over the next 36 h and moved into central Iowa by 2100 UTC 2 April 2010. The trailing cold front overtook the dryline in Iowa by 0300 UTC 3 April 2010. The 2100 UTC 2 April 2010 WPC surface analysis (Fig. 10a) shows this dryline over Iowa analyzed as a cold front. However, the characteristics of the boundary (mT air to its east and cT air to its west; Fig. 10b) suggest that this is actually a dryline and not a cold front as analyzed. Analysis of air parcel backward trajectories (Figs. 10c and 10d) confirms that the air mass to the west of the boundary was transported from the Mexican Plateau into southwestern Iowa. The boundary to the west is an arctic cold front separating a cP air mass from a cT air mass, confirmed by the air parcel backward trajectories indicating different source regions (Figs. 10c and 10d) and the surface observations showing strongly differing airmass characteristics (Fig. 10a).

The three examples presented here are not atypical—many drylines identified in this study have not been analyzed as such. Of the 33 cases for which WPC analyses were available (due to a limited archive), only 6 (18%) of identified MRV drylines were analyzed as drylines. Of the other cases, 13 (39%) were analyzed as cold fronts, 2 were analyzed as stationary or warm fronts, 5 were analyzed as a trough axis, and 7 were not analyzed as any type of boundary. There are also inconsistencies between official analyses of MRV drylines.

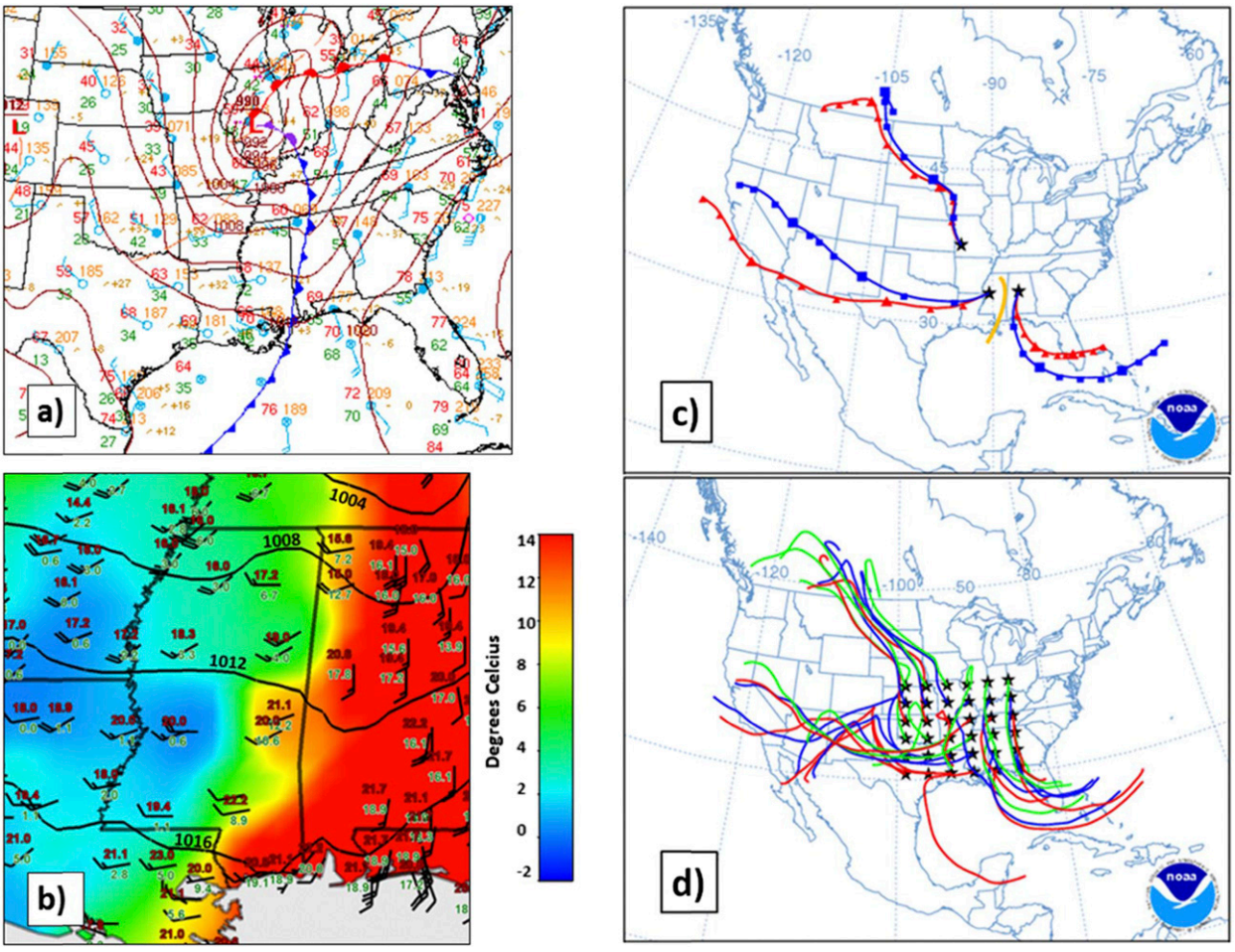

FIG. 9. (a)–(d) As in Fig. 8, but for 1800 UTC 11 Feb 2009. In (b), note the strong dewpoint gradient in western Alabama, with the increasing dewpoint northwest across Arkansas and Oklahoma.

Figures from the first and third examples in this section (24–25 February 2007 and 2 April 2010) are presented as an illustration of the inconsistencies in MRV dryline analysis between the Storm Prediction Center (SPC) and the WPC. Figure 11a is a graphic from the SPC Mesoscale Discussion 199, issued by the SPC at 2149 UTC 24 February 2007, showing a dryline in Arkansas and Louisiana. The WPC surface analysis valid at 0300 UTC 25 February 2007 (Fig. 8a) had the same boundary analyzed as a cold front. Inconsistent analysis appears again in the third example. SPC Mesoscale Discussion 0240 issued at 0101 UTC 3 April 2010 (Fig. 11b) indicates a dryline in Oklahoma and Texas, the same boundary that had been identified as a cold front farther north by the WPC at 2100 UTC 2 April 2010 (Fig. 10a). As shown earlier, the dryline did extend farther north into Iowa, but there were no mesoscale discussions valid north of Oklahoma. These cases illustrate the need for more consistent analysis of MRV dryline events.

As shown in section 3b, greater than half of MRV dryline events were associated with severe weather reports, and 15 (nearly 40%) were associated with tornado reports (often EF-2 or stronger). A seasonal bias could be assessed for winter (December–February) and spring (March–May); too few cases were available for other seasons. Springtime MRV drylines were associated with 4.1 times the number of severe wind and hail reports and 2.4 times the number of tornado reports compared to winter MRV drylines. We also examined how often boundaries were associated with severe weather reports as a function of how they were analyzed. Boundaries analyzed as drylines ($n = 6$) often contained a strong moisture gradient and appeared similar to a typical Great Plains dryline, and all were associated with large numbers of wind/hail reports and at least one tornado report. Two of these events were associated with a slight risk designation from the Storm Prediction Center in their 0600 UTC outlook on the morning of the dryline,

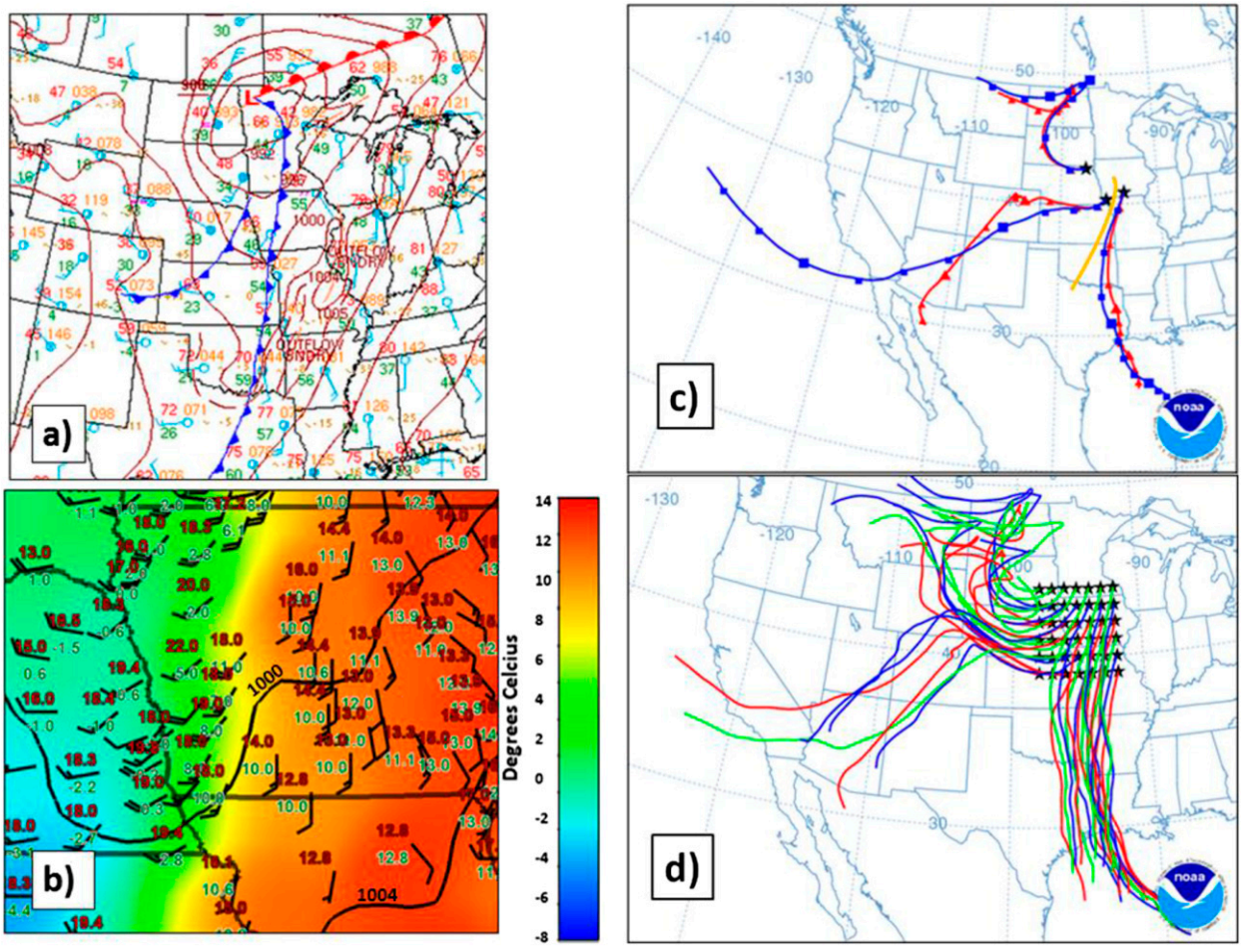

FIG. 10. As in Fig. 8, but for 2100 UTC 2 Apr 2010.

and both of these cases produced significant severe weather outbreaks (one produced 24 tornado reports, the other produced 87 wind/hail reports and 6 tornado reports). Thus, *the potential of strong MRV drylines to produce substantial severe weather outbreaks should not be underestimated*. MRV drylines analyzed as fronts (cold, warm, or stationary) produced severe weather reports in 21 (53%) events, consistent with the average across the whole dataset. MRV drylines analyzed as trough axes, or for which no boundary was analyzed, produced severe reports in 10 (25%) events. These results underscore the significance of MRV drylines for severe weather production, and indicate that even MRV dryline events with relatively weak moisture gradients are also occasionally associated with severe weather reports. From a nowcasting perspective, dynamics of convection initiation may be similar between storms initiated by MRV drylines and other types of boundaries such as cold fronts. Convection initiated by MRV drylines can be poorly anticipated, however, leading to unanticipated severe convection and/or smaller lead times. It is not known how convective mode and intensity vary between storms initiated by MRV drylines and those initiated by other types of boundaries—although these are important questions, they are beyond the scope of this work. Of primary importance here is to increase forecaster awareness of MRV drylines so there is better anticipation of associated convection initiation. This is particularly important given the often-volatile severe weather environment present in association with MRV drylines.

When drylines move east of the Great Plains, they may become more difficult to differentiate from cold fronts. Because of the synoptically active environments associated with these drylines, air parcels west of the surface dryline often can be shown to have been located over the eastern Pacific Ocean just a few days before moving into the eastern United States. These air parcel trajectories may cause some forecasters to identify these boundaries as Pacific cold fronts instead of drylines.

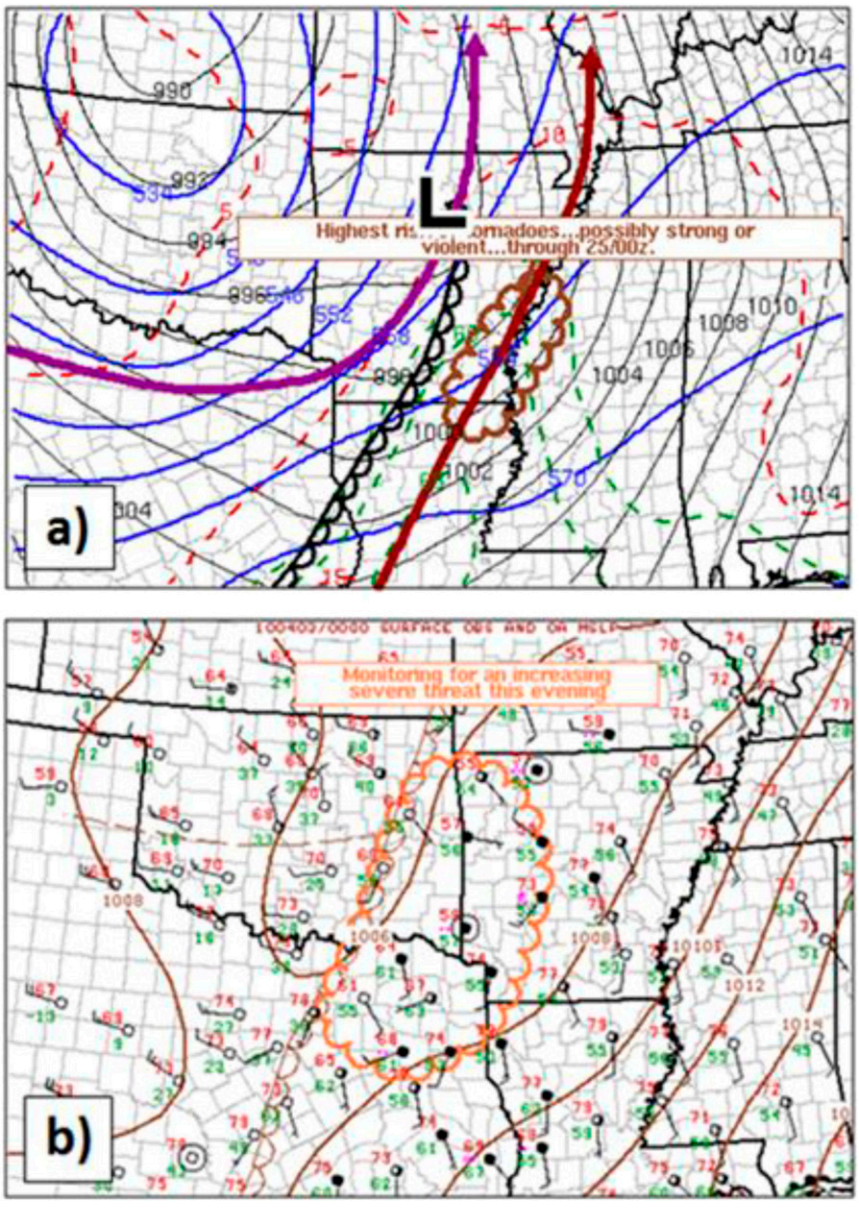

FIG. 11. (a) Storm Prediction Center mesoscale discussion issued at 2149 UTC 24 Feb 2007. (b) Storm Prediction Center mesoscale discussion issued at 0101 UTC 3 Apr 2010.

However, once the air parcels have moved over the Mexican Plateau, the air mass takes on the characteristics of a cT air mass with high temperature and low dewpoint.

Inconsistencies in the analyses of MRV drylines may also be partially explained by an expectation bias—forecasters may not be aware that drylines move east of the Great Plains. A hopeful outcome of this study is to increase awareness of these boundaries, leading to more consistent future analyses of MRV drylines. Additionally, the application of the classic Norwegian cyclone model to the central United States can result in dryline misanalysis. Through their study of multiple warm-front-like baroclinic zones in extratropical cyclones, Metz et al. (2004) demonstrated the deficiencies in applying a single conceptual model of cyclone structure and evolution to all cyclones in the central United States. A number of models of cyclones in the central United States have been proposed to account for the limitations of the application of the Norwegian cyclone model to the geography of the central United States. These cyclone models include a lee cyclone model

(Hobbs et al. 1996) and a cold front aloft cyclone model (Locatelli et al. 2002a), which account for nonclassical features such as drylines, dry troughs, and cold fronts aloft that are associated with cyclones in the central United States. It is important when performing surface analysis to be mindful that no one conceptual model of cyclone structure and evolution is adequate to represent the observed variety of cyclones in the central United States (Metz et al. 2004).

7. Summary

A study of Mississippi River valley drylines was completed in an effort to learn more about these boundaries and to ultimately increase forecaster awareness of drylines east of their typical domain. The primary conclusions of this study are as follows:

- In total 39 MRV drylines were identified between 1999 and 2013. Arkansas experienced the most MRV dryline passages, followed by Louisiana and then by Missouri.
- The peak in frequency of MRV drylines occurs earlier in the year (February–April) than the peak in frequency of southern Great Plains drylines.
- There is a weak correlation between observed dryline longitude and month of the year, with drylines moving farthest east during the winter months. The location of MRV dryline latitude shifted slightly northward throughout the winter and spring.
- For the sample of MRV drylines examined here, more than half were associated with severe weather reports, and approximately 40% were associated with at least one tornado report; many MRV dryline days with tornadoes had at least one EF2+ tornado.
- Amplified upper-air patterns were observed on the MRV dryline days, with the 250-hPa composite jet observed to the west, northwest, or southwest of the drylines. The strongest 250-hPa composite jet was observed for drylines in Mississippi and Alabama. A 500-hPa shortwave trough was generally located to the northwest of the drylines, with strong negative 500-hPa height anomalies across the central United States and positive height anomalies over the northeastern United States. Strong 850-hPa westerlies were generally centered to the west of the drylines. A strong surface cyclone was typically located poleward of the drylines, with the strongest surface cyclones observed for Mississippi and Alabama dryline events.
- Examination of surface maps for dryline days showed that only 18% of this study's identified MRV drylines were analyzed as drylines by the Weather Prediction Center. The analysis of MRV drylines was also found to be inconsistent between the Weather Prediction Center and the Storm Prediction Center.

Acknowledgments. The lead author was supported by a research assistantship at the University of Nebraska–Lincoln, and the coauthor was supported by an academic appointment. Drs. Adam Houston and Mark Anderson provided helpful guidance and insight throughout the project. Dr. David Schultz, Phil Bergmaier, and an anonymous reviewer provided reviews that substantially strengthened the manuscript. The Air Resources Lab (www.arl.noaa.gov) is acknowledged for providing HYSPLIT trajectories. The University of Wyoming provided archived upper-air observations (http://weather.uwyo.edu/upperair/sounding.html). WeatherScope software from the Oklahoma Climatological Survey (https://www.mesonet.org/index.php/weather/weatherscope) was used to generate plots of historic surface data (Figs. 8–10).

REFERENCES

Atkins, N. T., R. M. Wakimoto, and C. L. Ziegler, 1998: Observations of the finescale structure of a dryline during VORTEX 95. *Mon. Wea. Rev.*, **126**, 525–550, doi:10.1175/1520-0493(1998)126<0525:OOTFSO>2.0.CO;2.

Banacos, P. C., and M. L. Ekster, 2010: The association of the elevated mixed layer with significant severe weather events in the northeastern United States. *Wea. Forecasting*, **25**, 1082–1102, doi:10.1175/2010WAF2222363.1.

Carlson, T. N., S. G. Benjamin, G. S. Forbes, and Y.-F. Li, 1983: Elevated mixed layers in the regional severe storm environment: Conceptual model and case studies. *Mon. Wea. Rev.*, **111**, 1453–1474, doi:10.1175/1520-0493(1983)111<1453:EMLITR>2.0.CO;2.

Corfidi, S. F., S. J. Weiss, J. S. Kain, S. J. Corfidi, R. M. Rabin, and J. J. Levit, 2010: Revisiting the 3–4 April 1974 Super Outbreak of tornadoes. *Wea. Forecasting*, **25**, 465–510, doi:10.1175/2009WAF2222297.1.

Dos Santos Mesquita, M., N. G. Kvamstø, A. Sorteberg, and D. E. Atkinson, 2008: Climatological properties of summertime extra-tropical storm tracks in the Northern Hemisphere. *Tellus*, **60A**, 557–569, doi:10.1111/j.1600-0870.2008.00305.x.

Doswell, C. A., H. E. Brooks, and M. P. Kay, 2005: Climatological estimates of daily local nontornadic severe thunderstorm probability for the United States. *Wea. Forecasting*, **20**, 577–595, doi:10.1175/WAF866.1.

Draxler, R. R., 1999: HYSPLIT4 user's guide. NOAA Tech. Memo. ERL ARL-230, NOAA/Air Resources Laboratory, Silver Spring, MD, 46 pp.

——, and G. D. Hess, 1997: Description of the HYSPLIT_4 modeling system. NOAA Tech. Memo. ERL ARL-224, NOAA/Air Resources Laboratory, Silver Spring, MD, 24 pp.

——, and ——, 1998: An overview of the HYSPLIT_4 modeling system of trajectories, dispersion, and deposition. *Aust. Meteor. Mag.*, **47**, 295–308.

——, and G. D. Rolph, 2015: HYSPLIT—Hybrid Single Particle Lagrangian Integrated Trajectory Model. NOAA/Air Resources Laboratory, College Park, MD, accessed 11 February

2014. [Available online at http://www.arl.noaa.gov/HYSPLIT.php.]

Eichler, T., and W. Higgins, 2006: Climatology and ENSO-related variability of North American extratropical cyclone activity. *J. Climate*, **19**, 2076–2093, doi:10.1175/JCLI3725.1.

Geerts, B., 2008: Dryline characteristics near Lubbock, Texas, based on radar and West Texas Mesonet data for May 2005 and May 2006. *Wea. Forecasting*, **23**, 392–406, doi:10.1175/2007WAF2007044.1.

Hane, C. E., 2004: Quiescent and synoptically-active drylines: A comparison based upon case studies. *Meteor. Atmos. Phys.*, **86**, 195–211, doi:10.1007/s00703-003-0026-y.

——, H. B. Bluestein, T. M. Crawford, M. E. Baldwin, and R. M. Rabin, 1997: Severe thunderstorm development in relation to along-dryline variability: A case study. *Mon. Wea. Rev.*, **125**, 231–251, doi:10.1175/1520-0493(1997)125<0231:STDIRT>2.0.CO;2.

Hobbs, P. V., J. D. Locatelli, and J. E. Martin, 1996: A new conceptual model for cyclones generated in the lee of the Rocky Mountains. *Bull. Amer. Meteor. Soc.*, **77**, 1169–1178, doi:10.1175/1520-0477(1996)077<1169:ANCMFC>2.0.CO;2.

Hoch, J., and P. Markowski, 2005: A climatology of springtime dryline position in the U.S. Great Plains region. *J. Climate*, **18**, 2132–2137, doi:10.1175/JCLI3392.1.

Kalnay, E., and Coauthors, 1996: The NCEP/NCAR 40-Year Reanalysis Project. *Bull. Amer. Meteor. Soc.*, **77**, 437–471, doi:10.1175/1520-0477(1996)077<0437:TNYRP>2.0.CO;2.

Knupp, K. R., and Coauthors, 2014: Meteorological overview of the devastating 27 April 2011 tornado outbreak. *Bull. Amer. Meteor. Soc.*, **95**, 1041–1062, doi:10.1175/BAMS-D-11-00229.1.

Locatelli, J. D., R. D. Schwartz, M. T. Stoelinga, and P. V. Hobbs, 2002a: Norwegian-type and cold front aloft-type cyclones east of the Rocky Mountains. *Wea. Forecasting*, **17**, 66–82, doi:10.1175/1520-0434(2002)017<0066:NTACFA>2.0.CO;2.

——, M. T. Stoelinga, and P. V. Hobbs, 2002b: A new look at the Super Outbreak of tornadoes on 3–4 April 1974. *Mon. Wea. Rev.*, **130**, 1633–1651, doi:10.1175/1520-0493(2002)130<1633:ANLATS>2.0.CO;2.

Maddox, R. A., M. S. Gilmore, C. A. Doswell III, R. H. Johns, C. A. Crisp, D. W. Burgess, J. A. Hart, and S. F. Piltz, 2013: Meteorological analyses of the Tri-State tornado event of March 1925. *Electron. J. Severe Storms Meteor.*, **8** (1). [Available online at http://ejssm.org/ojs/index.php/ejssm/issue/view/43.]

Martin, J. E., J. D. Locatelli, P. V. Hobbs, P. Wang, and J. A. Castle, 1995: Structure and evolution of winter cyclones in the central United States and their effects on the distribution of precipitation. Part I: A synoptic-scale rainband associated with a dryline and lee trough. *Mon. Wea. Rev.*, **123**, 241–264, doi:10.1175/1520-0493(1995)123<0241:SAEOWC>2.0.CO;2.

Mesinger, F., and Coauthors, 2006: North American Regional Reanalysis. *Bull. Amer. Meteor. Soc.*, **87**, 343–360, doi:10.1175/BAMS-87-3-343.

Metz, N. D., M. Schultz, and R. H. Johns, 2004: Extratropical cyclones with multiple warm-front-like baroclinic zones and their relationship to severe convective storms. *Wea. Forecasting*, **19**, 907–916, doi:10.1175/1520-0434(2004)019<0907:ECWMWB>2.0.CO;2.

Miller, D. A., and F. Sanders, 1980: Mesoscale conditions for the severe convection of 3 April 1974 in the east-central United States. *J. Atmos. Sci.*, **37**, 1041–1055, doi:10.1175/1520-0469(1980)037<1041:MCFTSC>2.0.CO;2.

Mulqueen, K. C., and D. M. Schultz, 2015: Non-classic extratropical cyclones on Met Office sea-level pressure charts: Double cold and warm fronts. *Weather*, **70**, 100–105, doi:10.1002/wea.2463.

NOAA/National Centers for Environmental Information, 2015: Storm Events Database. NOAA/National Centers for Environmental Information. Subset used: February 1999-February 2013, accessed 11 May 2015.

Rhea, J. O., 1966: A study of thunderstorm formation along dry lines. *J. Appl. Meteor.*, **5**, 58–63, doi:10.1175/1520-0450(1966)005<0058:ASOTFA>2.0.CO;2.

Robinson, P. J., 1998: Monthly variation of dew point temperature in the coterminous United States. *Int. J. Climatol.*, **18**, 1539–1556, doi:10.1002/(SICI)1097-0088(19981130)18:14<1539::AID-JOC326>3.0.CO;2-L.

Rolph, G. D., 2015: READY—Real-time Environmental Applications and Display sYstem. NOAA/Air Resources Laboratory, Silver Spring, MD, accessed 11 February 2014. [Available online at http://www.ready.noaa.gov.]

Schaefer, J. T., 1974: The lifecycle of the dryline. *J. Appl. Meteor.*, **13**, 444–449, doi:10.1175/1520-0450(1974)013<0444:TLCOTD>2.0.CO;2.

——, 1986: The dryline. *Mesoscale Meteorology and Forecasting*, P. S. Ray, Ed., Amer. Meteor. Soc., 549–572.

Schultz, D. M., C. C. Weiss, and P. M. Hoffman, 2007: The synoptic regulation of dryline intensity. *Mon. Wea. Rev.*, **135**, 1699–1709, doi:10.1175/MWR3376.1.

Smith, P. L., 1999: Effects of imperfect storm reporting on the verification of weather warnings. *Bull. Amer. Meteor. Soc.*, **80**, 1099–1105, doi:10.1175/1520-0477(1999)080<1099:EOISRO>2.0.CO;2.

Steenburgh, W. J., and C. F. Mass, 1994: The structure and evolution of a simulated Rocky Mountain lee trough. *Mon. Wea. Rev.*, **122**, 2740–2761, doi:10.1175/1520-0493(1994)122<2740:TSAEOA>2.0.CO;2.

Trapp, R. J., D. M. Wheatley, N. T. Atkins, R. W. Przybylinski, and R. Wolf, 2006: Buyer beware: Some words of caution on the use of severe wind reports in postevent assessment and research. *Wea. Forecasting*, **21**, 408–415, doi:10.1175/WAF925.1.

Weiss, C. C., H. B. Bluestein, and A. L. Pazmany, 2006: Finescale radar observations of the 22 May 2002 dryline during the International H_2O Project (IHOP). *Mon. Wea. Rev.*, **134**, 273–293, doi:10.1175/MWR3068.1.

Ziegler, C. L., and E. N. Rasmussen, 1998: The initiation of moist convection at the dryline: Forecasting issues from a case study perspective. *Wea. Forecasting*, **13**, 1106–1131, doi:10.1175/1520-0434(1998)013<1106:TIOMCA>2.0.CO;2.